Elsevier Editorial System(tm) for European Journal of Pharmaceutics and Biopharmaceutics
Manuscript Draft

Manuscript Number: EJPB-D-16-00358R1

Title: Nanoformulations for dimethyl fumarate: physicochemical characterization and in vitro/in vivo behavior

Article Type: VSI: 25 Years SLN & NLC

Keywords: solid lipid nanoparticles; dimethyl fumarate; brain delivery; multiple sclerosis; in vivo biodistribution; fluorescent luminescence imaging

Corresponding Author: Professor Claudio Nastruzzi,

Corresponding Author's Institution: University of Ferrara

First Author: Elisabetta Esposito

Order of Authors: Elisabetta Esposito; Rita Cortesi; Markus Drechsler; Jie Fan; Bingmei M Fu; Laura Calderan; Silvia Mannucci; Federico Boschi; Claudio Nastruzzi

Manuscript Region of Origin: ITALY

Abstract: Dimethyl fumarate has been demonstrated useful in relapsing remitting multiple sclerosis treatment (Tecfidera®). Nevertheless, since Tecfidera® capsules induce flushing, gastro-intestinal events and other more serious drawbacks, in this investigation a nanoparticle based system to be administered by an alternative way is proposed. In particular this study describes the preparation and characterization of dimethyl fumarate-containing solid lipid nanoparticles (SLN). Namely SLN based on tristearin, tristearin SLN treated with polysorbate 80 and cationic SLN constituted of tristearin in mixture with dimethyldioctadecylammonium chloride were investigated. The effect of the presence of dimethyl fumarate, functionalization by polysorbate 80 and dimethyldioctadecylammonium chloride was studied on morphology and dimensional distribution of SLN, by photon correlation spectroscopy and cryogenic transmission electron microscopy. Dimethyl fumarate release from SLN, studied by Franz cell, evidenced a Fickian dissolutive type kinetic in the case of SLN treated by polysorbate 80. Moreover fluorescent SLN were produced and characterized in order to investigate their in vitro permeability and in vivo biodistribution in mice.
An in vitro study of fluorescent SLN permeability performed through a model of mouse brain microvascular endothelial cells, indicated that cationic SLN displayed higher permeability values with respect to neutral SLN and SLN treated by polysorbate 80. Biodistribution of polysorbate 80 treated SLN was studied by fluorescent imaging after intraperitoneal or intranasal administration in mice. The in vivo images indicate that polysorbate 80 treated SLN were able to reach the brain, even if they prevalently accumulated in liver and spleen, especially by intraperitoneal route.

Cover Letter

Prof. Dr. Rainer H. Müller
Freie Universität Berlin
Department of Pharmacy
Pharmaceutical Technology, Biopharmaceutics & NutriCosmetics
Kelchstraße 31
12169 Berlin, GERMANY

Enclosed please find the manuscript "Nanoformulations for dimethyl fumarate: physicochemical characterization and *in vitro/in vivo* behavior", by Elisabetta Esposito, Rita Cortesi, Markus Drechsler, Jie Fan, Bingmei M. Fu, Laura Calderan, Silvia Mannucci, Federico Boschi and Claudio Nastruzzi.

The paper is submitted following the invitation to participate at the special issue: "Lipid nanoparticles: SLN & NLC" for possible publication on “European Journal of Pharmaceutics and Biopharmaceutics”.

The manuscript regards the production, characterization, *in vitro* and *in vivo* evaluation of dimethyl fumarate containing SLN.
The manuscript is original, unpublished, it is not under consideration for publication elsewhere, and all authors have read and approved the text and consent to its publication.

I thank you in advance for consideration.
Best regards

Prof Claudio Nastruzzi

Ferrara, 29 april 2016

Cornelia M Keck, Dr. rer. nat.
Guest Editor
European Journal of Pharmaceutics and Biopharmaceutics

Ms. Ref. No.: EJPB-D-16-00358

Title: Nanoformulations for dimethyl fumarate: physicochemical characterization and in vitro/in vivo behavior

We thank the Editor and the Reviewers for their comments on our manuscript, we have revised the manuscript to accomplish with the Reviewers' requests.
The revisions made are below reported and highlighted in yellow in the manuscript file.

Reviewer #1

Point 1

As suggested, the abstract has been revised.

Point 2

The key words have been updated and implemented.

Point 3

The abbreviation FAE has been introduced where requested.

Point 4

Following the suggestion of the reviewer, the verb "treated" has been replaced by "incubated".

Point 5

The abbreviations LP and WP have been deleted and replaced by "lipid phase" and "water phase"

Point 6

The indications for the equipments used for emulsification and ultrasonication have been included.

Point 7
Table 1 is correctly cited in the text, before Table 2, precisely in the Materials and Methods section, paragraph 2.2 "Determination of dimethyl fumarate solubility" (line 1). In addition, Table 1 is also cited before Table 2 in the Results and Discussion section, paragraph 3.1. "Preparation of SLN" (line 5).

Point 8
Space before "controlled" has been removed.

Point 9
For clarity, in paragraph 2.10, Line 9, it has been specified that SLN/P80-e are non fluorescent nanoparticles, used as control.

Point 10
See point 7.

Point 11
In paragraph 3.1. "Preparation of SLN", the explanation about the use of Poloxamer 188 and Tween 80 has been provided.
Poloxamer 188 was employed as stabilizer of the O/W emulsion and its presence is mandatory in order to produced small (i.e. diameter < 350 nm) and homogeneous (SD < 30 nm) SLN.
On the other hand, Tween 80 was employed as surface modifier (PEGylating agent) for preformed SLN, not as emulsion stabilizer during the preparation.

Point 12
A comma has been removed.

Point 13
See point 7.

Point 14

The "dimensional distribution" has been replaced by "mean particle sizes and polydispersity indices".

Point 15
See point 5.

Point 16
The use of the term "recovery" has been clarified and stated in the text.

Point 17
"in this conditions" has been replaced by "in these conditions".

Point 18
Tween is with capital T.

Point 19
"the obtain data" has been replaced by "the obtained data".

Point 20
SLN/P80-e are non fluorescent nanoparticle, used as control, for background reasons.

Point 21
A further explanation about the biodistribution of SLN after in vivo administration by different routes has been provided.

Point 22
As already specified in point 20, SLN/P80-e are non fluorescent nanoparticle, used as control, for background reasons. We thank the reviewer for its suggestion, indeed we found a mistake in the manuscript, paragraph 3.8. "Biodistribution studies", with regard to the mention of Figures 7 and 8, we exchanged panel A with the mention of panel C. The text has been revised accordingly.

Point 23
In the revised manuscript the quantification of the SLN reaching the brain has been provided as new Fig. 9, accordingly the relative experimental method has been provided.

Point 24
"proved" has been replaced by "proven".

Reviewer #2

Point 1
The presence of polysorbate 80 in the aqueous phase of the water /ethanol mixture has been added.

Point 2
The determination of DMF solubility in molten tristearin was performed by visual inspection, detecting the limit of solubility by evaluating the presence of DMF crystals in the molten tristearin (paragraph 2.2).

Point 3
DMF resulted soluble up to 8 mg/100 mg of tristearin (paragraph 3.1).

Point 4
Literature data report that DDAC when tested in rats, exhibits very low acute toxicity with oral LD_{50} > 2,000 mg/kg, dermal LD_{50} > 2,000 mg/kg.
Considering that in SLN/DDAC-e the amount of DDAC is 10 mg/ml and the volume of administration for the i.n route is 50 μl, the amount of DDAC administered is therefore 20 mg/kg in mice, therefore the administered dose is 100 fold lower than LD_{50}.
In addition, the Summary Risk Assessment Report, produced in 2009 by Institute for Health and Consumer Protection, Former Toxicology and Chemical Substance European Chemicals Bureau, indicates that there was no lethality in rats at extremely high exposure levels (180,000 mg^3 for 1 hour). During normal use of DODMAC, occupational exposure at this extreme level can be excluded. Therefore acute inhalation risks are not considered of concern. Acute dermal toxicity is considered to be very low as well. There was no lethality at the dose level of 2,000 mg/kg. Percutaneous absorption is known to be very low. The highest value for dermal exposure was calculated to be 170 mg/person/d. Comparison of

this level of exposure with acute dermal toxicity data shows that acute dermal risks are not considered of concern.

Point 5
The stability of SLN formulations has been determined over 6 months. We found that SLN maintained mean diameter almost unvaried, a milky aspect and almost absence of phase separation or agglomeration. Paragraphs 2.7, 3.4, last lines of paragraph 3.6 and Figure 3 have been added in order to explain the obtained data.

Point 6
Table numbers have been corrected.

Point 7
The dispersity indices are reported in Figure 2A.

Point 8
With respect to the suitability of DMF loaded SLN for therapeutic use, a comment has been added to the "Conclusion" section.
Moreover, the use of the intranasal administration could solve some drawbacks associated to the oral administration of the DMF. For instance, Tecfidera may cause flushing, gastro-intestinal events and blood cell abnormality; in addition a nasal formulation represents a suitable alternative to oral capsules in order to overcome dysphagia problems often associated to MS.

Point 9
Psoriasis has been eliminated from the "Conclusions".

Point 10
References 31-33 have been inserted.

Point 11
References 38, 39, 40 have been emended.

Hoping the manuscript is now suitable for publication in European Journal of Pharmaceutics and Biopharmaceutics, I send my best regards.
Prof Claudio Nastruzzi

*Graphical abstract

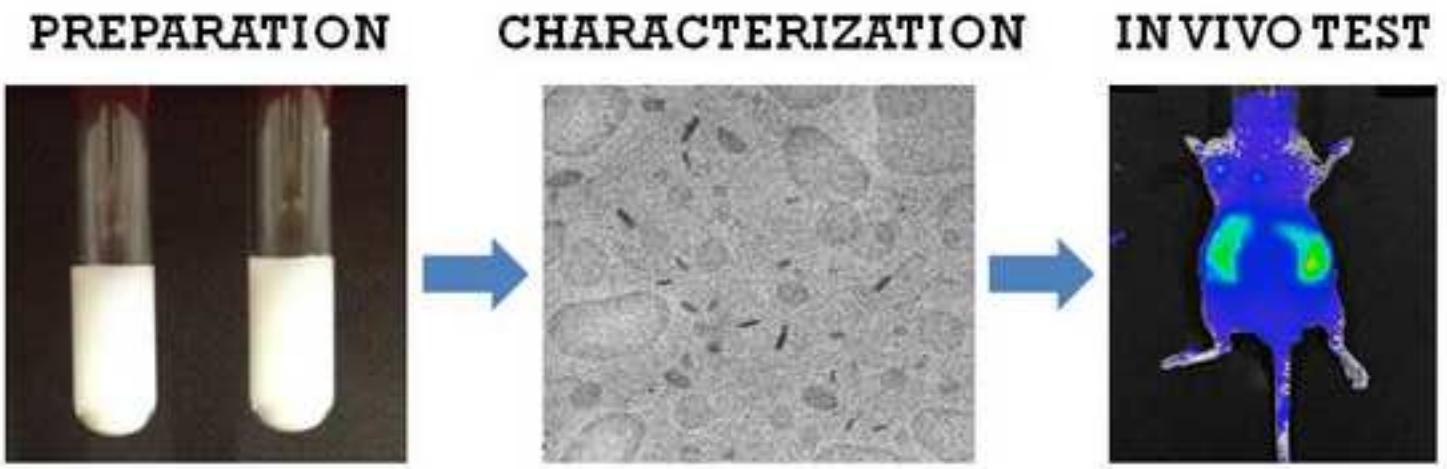

Nanoformulations for dimethyl fumarate: physicochemical characterization and *in vitro/in vivo* behavior

Elisabetta Esposito[a], Rita Cortesi[a], Markus Drechsler[b], Jie Fan[c], Bingmei M. Fu[C], Laura Calderan[d], Silvia Mannucci[d], Federico Boschi[e], Claudio Nastruzzi[a*]

[a]*Department of Life Sciences and Biotechnology, University of Ferrara, 44121 Ferrara, Italy*

[b]*BIMF / Soft Matter Electron microscopy, University of Bayreuth, Germany*

[c]*Department of Biomedical Engineering City University of New York, New York, NY 1003*

[d]*Department of Computer Science, University of Verona, 37134 Verona, Italy*

[e]*Department of Neurological and Movement Sciences, University of Verona, 37134 Verona, Italy.*

*Correspondence to: Prof Claudio Nastruzzi
Department of Life Sciences and Biotechnology
Via Fossato di Mortara, 19
I-44121 Ferrara, Italy
Tel. +39/0532/455348
e-mail nas@unife.it

ABSTRACT

Dimethyl fumarate has been demonstrated useful in relapsing remitting multiple sclerosis treatment (Tecfidera®). Nevertheless, since Tecfidera® capsules induce flushing, gastro-intestinal events and other more serious drawbacks, in this investigation a nanoparticle based system to be administered by an alternative way is proposed. In particular this study describes the preparation and characterization of dimethyl fumarate-containing solid lipid nanoparticles (SLN). Namely SLN based on tristearin, tristearin SLN treated with polysorbate 80 and cationic SLN constituted of tristearin in mixture with dimethyldioctadecylammonium chloride were investigated. The effect of the presence of dimethyl fumarate, functionalization by polysorbate 80 and dimethyldioctadecylammonium chloride was studied on morphology and dimensional distribution of SLN, by photon correlation spectroscopy and cryogenic transmission electron microscopy. Dimethyl fumarate release from SLN, studied by Franz cell, evidenced a Fickian dissolutive type kinetic in the case of SLN treated by polysorbate 80. Moreover fluorescent SLN were produced and characterized in order to investigate their *in vitro* permeability and *in vivo* biodistribution in mice.

An *in vitro* study of fluorescent SLN permeability performed through a model of mouse brain microvascular endothelial cells, indicated that cationic SLN displayed higher permeability values with respect to neutral SLN and SLN treated by polysorbate 80. Biodistribution of polysorbate 80 treated SLN was studied by fluorescent imaging after intraperitoneal or intranasal administration in mice. The *in vivo* images indicate that polysorbate 80 treated SLN were able to reach the brain, even if they prevalently accumulated in liver and spleen, especially by intraperitoneal route.

Keywords: solid lipid nanoparticles; dimethyl fumarate; brain delivery; multiple sclerosis; *in vivo* biodistribution; fluorescent luminescence imaging.

1. Introduction

Multiple Sclerosis (MS) is an inflammatory, progressive autoimmune disease that is a leading cause of disability in young adults. The mean age of onset is about 30 years [1]. MS is a debilitating disease, accompanied by neurological symptoms of varying severity, which over many years leads to accumulation of neurologic disability [1]. Current available therapies for MS are mainly focused on reducing the inflammatory effects of the disease [2]. However, the reduction of disease activity and particularly the reduction of disease progression are not always satisfactory and the more efficacious compounds may lead to serious side effects. There thus remains a high and unmet medical need for new efficacious and safe therapeutic approaches [2,3].

Interesting molecules employed in the treatment of MS are fumaric acid esters (FAE), such as dimethyl fumarate (DMF) [4].

FAE have been firstly employed to treat psoriasis, while recently DMF has been demonstrated useful in relapsing remitting MS, formulated as hard gelatin capsules, marketed as Tecfidera® [4-6]. DMF has a dual cytoprotective and immunosuppressive (anti-inflammatory) mechanism of action [7]. It is supposed to act by suppressing (a) the expression of cytokine and adhesion molecules implicated in the inflammatory response, and (b) NF-κB (nuclear factor kappa B)-dependent transcription, which regulates the expression of pro-inflammatory genes. Notably FAE stabilize Nrf2 and activate the Nrf2 pathway, which protects the blood–brain barrier (BBB) and support the maintenance of myelin integrity [7].

Despite Tecfidera® efficacy in MS, capsule administration causes flushing, gastro-intestinal drawbacks and other more serious side effects, including kidney disturbance and white blood cell abnormality [6, 7]. At the same time, Tecfidera® therapy requires two capsules a day for sustained efficacy, eventhough the oral administration is incompatible with the swallowing dysfunctions commonly observed in MS patients [8]. In this regard, a

nanocarrier to be administered by an alternative way would be desirable. This study focuses on the production and characterization of solid lipid nanoparticles (SLN) for DMF as new nanomedicines for MS.

SLN offer several advantages over conventional formulations, such as controlled release of the active molecule, the reduction of drug dosage and number of administrations, the possibility to target the brain and the immune system [9-14]. In addition SLN can be administered by non invasive routes, such as the intranasal, increasing patient compliance and decreasing gastro-intestinal events [15, 16].

In this study, in order to draw SLN suitable for DMF delivery through the brain, different strategies have been considered. Notably SLN were incubated with polysorbate 80 (P80) with the aim to modify nanoparticle surface. Notably, a proper modification of SLN surface has been reported as highly effective strategy to alter SLN biodistribution, enhancing blood circulation time and deposition in non-RES organs [17, 18].

In addition SLN were produced introducing in the lipid composition a cationic lipid, such as dimethyldioctadecylammonium chloride (DDAC), in order to confer a positive charge to SLN. Indeed it is known that a cationic surface on nanoparticle could facilitate the entrance through the BBB by electrostatic interaction [19, 20].

Moreover fluorescent SLN were designed, including different dyes specifically selected for studying *in vitro* permeation on mouse brain microvascular endothelial cells or *in vivo* biodistribution after intraperitoneal and intranasal administrations in mice. Particularly biodistribution was evaluated by fluorescence luminescent imaging, a non-invasive way to evaluate nanoparticle biodistribution, allowing to detect, visualize and quantify fluorescence all over the body of living animals [21].

2. Materials and Methods

2.1 Materials

The copolymer poly (ethylene oxide) (a) –poly (propylene oxide) (b) (a=80, b=27) (poloxamer 188) was a gift of BASF ChemTrade GmbH (Burgbernheim, Germany). Tristearin, stearic triglyceride (tristearin), dimethyldioctadecylammonium chloride (DDAC), polysorbate 80 (P80), dimethyl fumarate (DMF), 5(6)-Carboxy-X-rhodamine (rhodamine, RH) and indocyanine green (cardiogreen, CG) were purchased from Sigma-Aldrich, Merck (Darmstadt, Germany).

2.2 Determination of dimethyl fumarate solubility

Solubility of DMF (see Table 1 for physico-chemical properties) in water, ethanol, water/ethanol mixtures and aqueous solution of polysorbate 80 (1% w/w)/ethanol mixtures was determined by saturating each solvent or solvent mixture with an excess of DMF. The obtained saturated solutions were moved overnight in a horizontal shaker (100 rpm; 37 ± 0.5ºC). At the end of the experiment 1 ml of samples were withdrawn and filtered through a Millex-LCR Filter, 0.45 µm, Hydrophilic PTFE, 25 mm (Millipore-Sigma-Aldrich Merck, Darmstadt, Germany) which has no absorption for DMF. Concentration of DMF was determined by RP-HPLC analysis.

HPLC analysis was carried out by an Agilent Zorbax Eclipse XBD-C18 column (Agilent Technologies, United States) (15 cm×0.46 cm) stainless steel packed with 5 µm particles, eluted at room temperature with a mobile phase consisting of a mixture of acetonitrile, water 25:75 v/v, at a flow rate of 1 ml/min. The UV-Vis detector was set at 220 nm. Two hundreds of filtered samples were diluted with mobile phase to a final volume of 1 ml, then 50 µl were injected into the HPLC system and compared with a DMF standard of known concentration.

Analyses were conducted in triplicate, mean and standard deviations values were calculated.

The determination of DMF solubility in molten tristearin was performed by visual inspection, detecting the limit of solubility by evaluating the presence of DMF crystals in the molten tristearin.

2.3 Production of SLN

SLN were prepared by melt and ultrasonication, following a previously reported method with minor modifications [22]. The lipid phase (5% with respect to the whole weight of the dispersion) was constituted of pure tristearin or a mixture of tristearin and DDAC in a 4:1 w/w ratio. Briefly, an aqueous poloxamer 188 solution (2.5 % w/w) heated at 80°C was added to the molten lipid phase, afterwards the mixture was emulsified at 15000 rpm, 80°C for 1 min (Ultra Turrax T25, IKA-Werke GmbH & Co. KG, Staufen, Germany), subjected to ultrasonication at 6.75 kHz for 15 min (Microson TM, Ultrasonic cell Disruptor) and then let cooling at 25 °C. SLN dispersions were stored at room temperature. In some cases, P80 (16.6% w/w with respect to the lipid weight) was added to the dispersion after the ultrasonication step, during cooling (at 40°C) and left under stirring (250 rpm) for 30 min. In the case of DMF containing SLN, the drug (0.1 % w/w) was added to the molten lipid phase before adding the aqueous poloxamer 188 solution. In the case of fluorescent SLN, the fluorescent dyes (RH and CG) were added to the molten lipid phase (0.4% w/w) before adding the aqueous poloxamer 188 solution. The purification of fluorescent SLN from free fluorescent dye and the determination of fluorescence content in SLN were performed as previously reported [21].

Table 2 reports the acronyms used throughout the text to indicate the different nanoparticles and their compositions.

2.5 Characterization of SLN

The macroscopic aspect of SLN was evaluated by visual inspection of 2 ml of SLN in 10 mm diameter glass vials at the distance of 30 cm, to detect possible phase separation, aggregation and sedimentation phenomena. The agglomerates of lipid phase occurring in some cases after SLN cooling were accurately weighed, after collection by small tweezers.

2.5.1 Cryogenic transmission electron microscopy (cryo-TEM) analysis

Samples were vitrified as previously described [23]. The vitrified specimen was transferred to a Zeiss EM922Omega transmission electron microscope for imaging using a cryoholder (CT3500, Gatan). The temperature of the sample was kept below -175 °C throughout the examination. Specimens were examined with doses of about 1000-2000 e/nm^2 at 200 kV. Images were recorded digitally by a CCD camera (Ultrascan 1000, Gatan) using an image processing system (GMS 1.9 software, Gatan). In addition size distribution of nanoparticles was performed by measuring 1000 nanoparticles for each cryo-TEM image by the digital analyzer ImageJ 1.48v.

2.5.2 Photon Correlation Spectroscopy (PCS) analysis

Submicron particle size analysis was performed using a Zetasizer 3000 PCS (Malvern Instr., Malvern, England) equipped with a 5 mW helium neon laser with a wavelength output of 633 nm. Glassware was cleaned of dust by washing with detergent and rinsing twice with water for injections. Measurements were made at 25 °C at an angle of 90°. Data were interpreted using the “CONTIN” method [24].

2.6 Encapsulation efficiency and loading capacity of SLN

The encapsulation efficiency (EE) and loading capacity (LC) of SLN were determined as previously described [25]. 100 µl aliquot of each SLN batch was

loaded in a centrifugal filter (Microcon centrifugal filter unit YM-10 membrane, NMWCO 10 kDa, Sigma Aldrich, St Louis, MO, USA) and centrifuged (Spectrafuge™ 24D Digital Microcentrifuge, Woodbridge NJ, USA) at 8,000 rpm for 20 min. The amount of DMF was determined after dissolving the lipid phase with a known amount of ethanol (1:10, v/v) by high performance liquid chromatography (HPLC), as above reported. EE and LC were determined following equations (1) and (2), respectively.

$$EE = L_{DMF} / T_{DMF} \times 100 \quad (1)$$

$$LC = L_{DMF} / T_{\text{lipid phase}} \times 100 \quad (2)$$

where L_{DMF} is the amount of DMF loaded in SLN, T_{DMF} stands for the total amount of DMF added to the formulation and $T_{\text{lipid phase}}$ for the total weight of lipid phase in the formulation. Determinations were performed six times in independent experiments and the mean values ± standard deviations were calculated.

2.7 Stability of SLN

Stability studies were conducted on SLN stored for 180 days at room temperature, routinely evaluating the macroscopic aspect (by visual inspection) and the dimensional characteristics of SLN (by PCS analysis). Size distribution was analyzed in triplicate after 90 and 180 days from SLN preparation.

2.8 In vitro release kinetics

In vitro release studies were performed using modified Franz diffusion cell [26-28]. Dialysis membrane having pore size 2.4 nm, molecular weight cutoff between 12,000–14,000, was used. Before mounting in a Franz diffusion cell, dialysis membranes were soaked in double-distilled water for 12 h. SLN

dispersions (1 ml) were placed in the donor compartment, the receptor compartment was filled with 5 ml of receiving phase, constituted of water/ethanol (90:10, v/v) in which 1%, w/w of P80 was dissolved [28]. During the experiments, the receiving phase was maintained under magnetic stirring at 500 rpm and at a temperature of 37 ± 1°C. At fixed time intervals, 100 μl of the sample was withdrawn from receiver compartment through side tube. Fresh receiving mixture was placed to maintain constant volume. Samples were analyzed by HPLC method as described below. The DMF concentrations were determined six times in independent experiments and the mean values ± standard deviations were calculated.

2.8.1 Drug release data analysis

The experimental release data obtained by the release experiments were fitted to the following semi-empirical equations respectively describing Fickian dissolutive (3) and diffusion (4) release mechanisms [29, 30]

$$Mt / M\infty = K_{Diss}\, t^{0.5} + c \quad (3)$$

$$1 - Mt / M\infty = e^{-Kdiff}\, t + c \quad (4)$$

where Mt / M∞ is the drug fraction released at the time t, (M∞ is the total drug content of the analyzed amount of SLN), K and c are coefficients calculated by plotting the linear forms of the indicated equations. The release data of percent of released drug (0-3 hours) were used to produce theoretical release curves.

2.9 In vitro permeability experiments

The mouse brain microvascular endothelial cells (bEnd.3, ATCC, Manassas, VA) were cultured in Dulbecco's Modified Eagle's Medium/Nutrient Mixture F-12 Ham (DMEM/F-12, Sigma-Aldrich, St. Louis, MO) supplemented with 10% fetal bovine serum (FBS, Atlanta Biologicals, Flowery Branch, GA), 2 mM L-

glutamine (Sigma-Aldrich, St. Louis, MO), 100 U/mL penicillin and 1 mg/mL streptomycin (Sigma-Aldrich, St. Louis, MO). Cells were incubated in the humidified atmosphere with 5% CO_2 at 37 °C.

The bEnd.3 cells (600 cells/mm^2) were placed on the 50 µg/mL fibronectin coated transwell filter (0.4 µm pore, Corning, Corning, NY) and cultured in cell culture medium for approximately 4 days until confluent. Then the culture medium was replaced with 1% BSA-Ringer solution (Ringer) as permeability measurement samples. Briefly, fluorescent SLN-RH, SLN/P80-RH or SLN/DDAC-RH in Ringer (1:10 dilution) were added to the upper chamber of the transwell while only Ringer was added to the bottom chamber; every 30 min of totally 120 min, a 150 µL of sample solution was collected from the bottom chamber, and the concentration of SLN-RH was determined by the plate reader (Bio-Tek, Winooski, VT) with the Ex/Em wavelengths of 530/590 nm. The permeability of the endothelial monolayer to SLN was calculated following equation (5).

$$P_{SLN} = \frac{\Delta C/\Delta t}{C_0} \cdot \frac{V}{A} \quad (5)$$

where ΔC/Δt is the increase rate of SLN concentration in the bottom chamber during the time interval Δt, C_0 is the SLN concentration in the upper chamber (assumed to be constant during the measurement), V is the volume of solution in the bottom chamber, and A is the surface area of the endothelial monolayer [31, 32]. The experiments were performed three times and the mean values ± standard deviations were calculated.

2.10 Biodistribution studies

Male, athymic mice (n = 12) (Harlan Laboratories, Italy), about 4-5 weeks old and 25 g in weight, were housed in a temperature- and humidity-controlled

environment, having free access to mouse chow and tap water. Animals were handled accordingly with the regulations of the Italian Ministry of Health and to the European Communities Council (86/609/EEC) directives. Mice were divided into three groups, the first group (n=4) was administered by an intraperitoneal injection with 500 µl of fluorescent SLN/P80-CG; the second group (n=4) was administered by an intranasal administration with 50 µl of fluorescent SLN/P80-CG; the third group (n=4) was administered by an intraperitoneal injection with 500 µl of non fluorescent SLN/P80-e, as control. Mice were imaged 4 hours after lipid nanoparticle injection. Optical images were acquired with IVIS Spectrum (Perkin Elmer, Massachusetts, United States) in fluorescent modality with excitation filter 740 nm and emission filter 800 nm. Other parameters were: exposure time 1 s, binning B=4, f/stop= 2. After the last acquisition, mice were sacrificed through an anaesthetic overdose and they were perfused with solutions of phosphate buffer saline and paraformaldehyde. After perfusion liver, brain, lungs, kidney, spleen and brown fat were extracted and imaged with the same parameters of the *in vivo* acquisitions.

Quantification of the fluorescence emission was done on the acquired optical images, tracing manually a region of interest corresponding to the anatomical brain region for *in vivo* acquisitions and a squared region of interest around the brain in case of the isolated organ. Statistical analysis was performed using standard routines of MATLAB (Mathworks). Multiple comparisons were performed by one-way ANOVA; differences between two groups were determined by Student's t-test.

3. Results and Discussion

3.1. Preparation of SLN

In order to assess the suitability of DMF for encapsulation in SLN, a physico-chemical characterization of the drug was performed, particularly focusing on its solubility behavior. In this respect, different solvents were considered, the relative results, summarized in Table 1, indicate that DMF is slightly soluble in water and sparingly soluble in ethanol or water/ethanol mixtures [33].

Moreover DMF resulted soluble up to 28 mg/100 mg of molten tristearin.

Thus DMF is suitable for the encapsulation in SLN, resulting in the formation of matrix type nanoparticles (i.e. those in which the drug is molecularly dispersed into the material forming the SLN) [9, 34].

With respect to the preparation procedure, SLN were produced by a two-step protocol based on the initial (step 1) emulsification of a molten lipid phase in a water phase containing the polymeric surfactant poloxamer 188 as stabilizer.

Notably, the presence of surfactant poloxamer 188 used as stabilizer of the O/W emulsion, is mandatory in order to produced small (i.e. diameter < 350 nm) and homogeneous (SD < 30 nm) SLN.

SLN produced with P80 as an alternative to poloxamer 188 were indeed extremely irregular in shape and size, with the presence of a large proportion of agglomerates (> 25%, as loss of lipid phase) due to a partial coalescence of lipid phase during the formation of the O/W emulsion. After cooling, the coalesced lipid phase appeared as a small flake floating on the surface of the SLN dispersion.

The emulsification was conducted under high speed mechanical stirring, followed by step 2, in which the formed emulsion was homogenized by ultrasonication treatment [22].

In an attempt to ameliorate the delivery performances of SLN, with specific regard to the delivery of DMF to brain, the modification of SLN surface with P80 was considered.

P80 was selected since it possesses a well-recognized stealth effect and it plays a specific role in brain targeting [35]. Notably, the coating of nanoparticles with polyethylene glycol (PEG) chains results in the formation of a structure that can "mask" the nanoparticles from the host's immune system, reducing RES capture and prolonging the circulatory time. Indeed, unmodified nanoparticles are usually captured by opsonins and subsequently eliminated from the body by phagocyte cells [37]. In addition it is supposed that P80 is able to inhibit the transporter P-glycoprotein that plays a role in the efflux of a wide range of endogenous and exogenous compounds across biological membranes, including BBB [36].

The coating of SLN with P80 was performed by a minor modification of a previously developed protocol [14, 21]. Notably, SLN were treated with P80, added immediately after step 2 (i.e. ultrasonication), as soon as the temperature fell down at 40°C. By this procedure, the coating of SLN is accomplished through the penetration of the surfactant hydrophobic chain within the not-yet-completely consolidated lipid matrix, during the cooling process. Therefore, whilst the lipophilic portion of P80 acts as a lipid anchor, the hydrophilic portion of P80, namely the PEG chains, protrude out from the SLN surface into the water phase, shielding and protecting the SLN from the environment (or viceversa). Therefore, P80 was employed as surface modifier (PEGylating agent) for preformed SLN, not as emulsion stabilizer during the preparation.

It is important to underline that, in spite of the positive effect on targeting and long-circulation time, PEGylation causes also alterations in the physiochemical properties of SLN, including hydrophobicity and hydrodynamic dimension.

In order to propose an alternative approach to PEGylation for brain targeting, possibly solving the problem related to the increase of dimension, cationic SLN were also produced.

The rationale of producing cationic SLN relies on the fact that brain microvasculature endothelia present a luminal electrostatic barrier at physiologic pH. In particular the surface expression and adhesion of the glycocalyx residues such as proteoglycans, sulfated mucopolysaccharides, sulfated, sialic acid-containing glycoproteins and glycolipids confer a negative electrostatic charge to specific area of the BBB [19, 38].

In this respect, cationic molecules filling anionic area on the BBB are able to penetrate probably by adsorptive mediated endocytosis or tight junction disruption process [19, 39, 40].

Similarly to this physiologic condition, in vitro studies have evidenced an electrostatic interaction between nanoparticles and BBB endothelia, in particular positively charged nanoparticles can interact with BBB better then anionic or neutral nanoparticles [19, 41].

In the case of cationic SLN, the inclusion of the cationic lipid was achieved by a different approach with respect to PEGylation. Cationic SLN were indeed obtained using a lipid molten mixture constituted of tristearin and DDAC.

Table 2 reports the composition of nanoparticles and the SLN acronyms employed throughout the text.

3.2. Characterization of SLN

The characterization of drug delivery systems, such as nanoparticles, is of paramount importance since physical properties such as morphology, size and size distribution can influence quality control, stability evaluation and biological fate.

For this reason, the effect of DMF, P80 treatment and DDAC was evaluated on SLN morphology, dimensional distribution, recovery and drug encapsulation efficiency.

The top of Fig. 1 reports images showing the macroscopic aspect of different SLN obtained in the absence (left) or in the presence (right) of DMF. SLN and

SLN/P80 appear milky, while SLN/DDAC are more translucent, suggesting smaller dimensions; the presence of DMF does not affect the macroscopic aspect with respect to the empty counterparts. Notably, no phase separation and sedimentation phenomena occurred in all SLN samples.

A more detailed analysis of SLN morphology was obtained by cryo-TEM; microphotographs, reported in Fig. 1, evidence the aspect of SLN and SLN/P80 or SLN/DDAC, in the absence and in the presence of DMF. In all cases SLN look like discoid structures that, when edge-on viewed, appear as electron dense “needles", indeed lipids tend to crystallize in non-spherical platelet form [22, 42]. Notably, cryo-TEM analysis indicated that SLN morphology was not influenced by P80 treatment or DDAC presence. Moreover the inclusion of DMF did not affect SLN structure.

The mean particle sizes and dispersity indices, reported in Table 2 and Fig. 2A, show that the diameters of SLN (expressed as Z Average) were comprised between 185 and 300 nm, particularly, SLN/P80 displayed the larger mean diameters and SLN/DDAC the smaller ones. The large dimensions found for SLN/P80 were explained by the presence of PEG around the SLN core, forming a “crown” of hydrophilic chains around nanoparticles. On the other hand, in the case of SLN/DDAC, the presence of DDAC molecules, decreasing the interfacial tension, facilitated the emulsification of the lipid phase into the water phase. This favored the formation of small nano-droplets, finally resulting in small nanoparticles after consolidation of the lipid phase. Moreover, the presence of the positively charged ammonium chloride portion of DDAC on the surface of SLN conferred a positive charge to the nanoparticles that increased the electrostatic repulsion between particles, avoiding agglomeration phenomena.

In all cases, the loading of SLN with DMF caused a slight increase of the particle mean diameter. The dispersity indices of all SLN were comprised between 0.16 and 0.28, indicating that the used production strategy resulted in the formation of uniform particles in term of dimensional distribution.

The % recovery of SLN (expressed as the amount of SLN recovered (g)/amount of lipid used (g) x 100) shown in Fig. 2B, was always very high in the case of empty formulation, with a very low presence of agglomerates; especially for SLN/DDAC, that displayed a percentage of agglomerates below 1 %.

In the case of formulations including the drug, the recovery was slightly lower; SLN-DMF and SLN/P80-DMF presented indeed a larger amount of agglomerates, causing a partial lipid lost. On the contrary, in SLN/DDAC-DMF the presence of DMF did not cause a significant reduction of the recovery, that was ≥ 97 % w/w.

3.3. Encapsulation efficiency and loading capacity of SLN

With the aim to obtain information on the main formulation characteristics, quantification of EE, LC (reported in Table 2) and release kinetics (reported in Fig. 3) were performed.

Initially, for the encapsulation of DMF in SLN, 20 μg of drug/mg lipid phase were added to the molten lipid phase. In these conditions, the encapsulation efficiency was found to be quite satisfactory, with an EE of about 85% for all the formulations tested, without any appreciable difference in the case of SLN treated with P80 or containing the cationic surfactant DDAC.

In the attempt to produce SLN containing a larger amount of DMF, the effect of different contents of DMF was tested, namely the amount of DMF was increased to 40, 60 and 80 μg of drug/mg lipid phase.

In Table 3 are summarized the obtained data, showing that by increasing the amount of DMF two unwanted effects occurred. For instance, a progressive decrease on SLN recovery, attributed to the formation of a high proportion of agglomerates due to the coalescence of the molten lipid droplets. A further consequence of the increased DMF content was the decrease in EE.

With respect to the encapsulation in SLN, our data indicate that when DMF was loaded up to 40 μg of drug/mg lipid phase, the EE remained quite high (> 80%),

on the contrary when DMF exceeded this amount (i.e. 60 and 80 μg of drug/mg lipid phase), the EE dropped rapidly to unsatisfactory values below 55%.

These data suggested that when the drug was added above a critical limit, the percentage of drug lost into agglomerates during encapsulation rapidly raised.

The percentage of encapsulated DMF with respect to the total lipid phase (expressed as LC) therefore remained relatively low, even when the highest DMF amount was employed.

It is to be underlined that the EE and LC values found in the case of DMF are in agreement with those obtained for other drugs encapsulated in the same experimental conditions and lipid composition [22, 43]. Similar results were also obtained when the lipid composition of nanoparticles was modified in order to produce nanostructured lipid carriers (NLC); indeed the presence of lipids leading to a an imperfect and disordered lipid matrix (e.g. caprylic/capric triglycerides) did not ameliorate the EE and LC, that remained relatively low, i.e. 33.4% and 0.4% respectively.

As a consequence we chose to employ SLN containing 20 μg of DMF/mg lipid phase for in vitro release studies.

3.4. Stability of SLN

Since stability is an important parameter to assess the actual potential of SLN as drug delivery systems, the variations on the general aspect of SLN suspension and nanoparticle size have been considered. Both parameters were investigated along a six month period of SLN storage at room temperature. When analyzed by visual inspection, all formulations maintained a homogeneous milky aspect, without any sign of phase separation or agglomeration phenomena. Moreover, the PCS dimensional analysis (reported in Fig. 3) revealed very low variations (≤10 nm) in the Z-average diameter of the SLN, indicating that all nanoparticle resulted very stable in term of dimensions.

3.5. In vitro release kinetics of DMF from SLN

The release profiles of DMF from SLN-DMF, SLN/P80-DMF and SLN/DDAC-DMF were determined in vitro by a Franz cell method. Since DMF is scarcely soluble in water (Table 1), in order to establish sink conditions the experiments were conducted using a receptor phase constituted of water/ethanol (90:10, v/v) containing 1%, w/w of Tween 80 as dispersing solubilizing agent [26].

From the analysis of the release data reported in Fig. 4, some considerations can be done: (a) irrespectively of their composition, the kinetic from nanoparticles was characterized by a initial fast release period (up to 2 hours) in which the drug release is almost linear, followed by a slower portion of the release profile, (b) all nanoparticles displayed a slower release with respect to the free drug and (c) only minor differences in the release profiles were found among the different tested SLN; a slightly faster release was associated to SLN treated with P80 (SLN/P80-DMF).

With the aim to evaluate if the mechanism of DMF release from SLN was predominantly governed by a dissolutive or diffusive model, a mathematical analysis of the release profile was performed. Namely, DMF theoretical release profiles were determined according to the linear form of Eq.(3) and Eq.(4). Thereafter a comparison between the theoretical and experimental DMF release profiles from nanoparticles was performed.

Fig. 5 reports data relative to SLN-DMF (Fig. 5A), SLN/P80-DMF (Fig. 5B) and SLN/DDAC-DMF (Fig. 5C); the kinetic parameters, determined by linearization of release rate data, are also reported in Table 4.

In the case of SLN-DMF and SLN/DDAC-DMF the experimental curves were almost superposable to the theoretical curves calculated from equations (3) and (4), suggesting a mixed kinetic with a combination of both dissolutive and diffusive release [30].

On the contrary, as shown in Fig. 5B, SLN/P80-DMF displayed a drug release more consistent with a dissolutive rather than of diffusive process, as proven by

the higher value of R found in the case of linearization of Eq.(3). In this case, the release of DMF appears predominantly governed by a non-Fickian mechanism, probably because of the presence of the PEG shield.
Generally, it can be concluded that the release of DMF from SLN is in large part a combination of Fickian diffusion and non-Fickian dissolution mechanisms, such as erosion and relaxation [30].

3.6. Production of fluorescent SLN

In order to produce fluorescent SLN for *in vitro* uptake and *in vivo* biodistribution studies, two fluorescent molecules were employed because of technical and methodological reasons. Indeed the fluorimeters require fluorophores characterized by different excitation and emission wavelengths. For *in vitro* studies, it is required a fluorescent molecule with an excitation wavelength at 560 nm and an emission at 590 nm, while for *in vivo* studies fluorescent molecules with an excitation wavelength at 740 nm and an emission at 800 nm are required to take advantage of the near infrared transparency window of the biological tissues. Accordingly, RH was selected for *in vitro* experiment while CG was chosen for *in vivo* studies.
The stability of the association between fluorescent dye and SLN was determined by thin layer chromatography experiments, indicating that the fluorescent probes were stably bound to the nanoparticles [21].
In the case of fluorescent SLN, the presence of the fluorescent dyes RH and CG resulted in milky dispersions respectively pink or green colored [21]. Importantly, the presence of RH and CG did not affect the morphology and scarcely influenced mean diameters of SLN (Table 2) [21].
Stability studies demonstrated that fluorescent SLN resulted very stable up to 6 months from production, in the presence and in the absence of DDAC or P80. Indeed fluorescent SLN did not display phase separation or agglomeration phenomena and maintained mean diameters below 195 nm [21].

3.7. In vitro permeability experiments

In order to determine the ability of nanoparticles to pass through the BBB, an *in vitro* model of the mouse BBB, was employed. The model was based on immortalized mouse brain endothelial cell line, bEnd3, chosen since this type of cells rapidly forms monolayer and possesses consistent BBB characteristics over repeated passages.

As preliminary experiment, the SLN-RH stability was tested in culture medium, determining the linearity between nanoparticle concentration and fluorescence emission. Fig. 6 shows the values obtained in permeability experiments, employing SLN-RH, SLN/P80-RH and SLN/DDAC-RH. The obtained data indicate that the presence of P80 did not increase the permeability of SLN through the *in vitro* BBB barrier, at least on the employed cellular model. Whereas DDAC presence slightly increased the permeability of SLN through bEnd.3 cells, showing a mean value 1.55 fold higher with respect to the corresponding neutral control nanoparticles. This result was attributed to the effect of the positive charge present on SLN/DDAC-RH, favoring the electrostatic interactions of SLN with the negatively charged endothelial cells [44, 45].

3.8. Biodistribution studies

A still open question about the use of SLN as tool for specialized drug delivery to the brain, relies on their *in vivo* biodistribution. Indeed the comprehension of the *in vivo* absorption, distribution and organ accumulation is crucial to ensure the efficacy and safety of SLN for clinical applications [46].

In this regard, the *in vivo* biodistribution of SLN was determined in experiments performed after intraperitoneal and intranasal administrations in athymic mice.

As animal model, athymic nude mice were chosen since these animals do not present fur and hear bulbs that are high absorbers and sources of light scattering. Nude mice allow indeed the detection of faint light signals coming from deepest anatomical districts.

In order to use an exiguous number of animals for ethical and cost reasons, we decided to perform a preliminary study, employing only SLN/P80-CG due to the P80 well-recognized stealth effect and specific role in brain targeting [17, 35, 37]. Intraperitoneal administration was selected since it is easy, safe and reproducible, moreover the peritoneal wall is rich in vessels, so intraperitoneal route is largely used for the systemic administration of drugs for animal study. It is well established that drugs and SLN injected by intraperitoneal route can reach all tissues and organs following the systemic blood circulation.

Specifically, by the intraperitoneal route, similarly to the oral route, SLN get into the systemic circulation mostly through hepatic portal system. The only difference is in the absorption phase, indeed by oral administration the substances are absorbed in the gastrointestinal tract, while by intraperitoneal route they diffuse across the peritoneal membrane, which is lined with a capillary bed. The blood vessels supplying and draining the abdominal viscera, musculature and mesentery, constitute a blood filled compartment into which drugs can rapidly diffuse from the peritoneum. Therefore, drugs administered by intraperitoneal route generally reach the systemic circulation more rapidly than those taken orally.

As an alternative to intraperitoneal administration, the i.n administration route was also selected with the aim to decrease gastro-intestinal events often associated to Tecfidera® capsule administration and increasing patient compliance. The intranasal route is non-invasive and rapid; by this route SLN could reach the central nervous system (specifically the brain) by two ways: (i) through direct olfactory transport, along the olfactory and trigeminal nerves pathways, bypassing in this way the BBB or (ii) through systemic circulation pathway via the transmucosal absorption [13, 14, 21].

The nanoparticle biodistribution was determined by a preclinical research method based on non-invasive *in vivo* fluorescent luminescent imaging of small animals [21]. Notably this technique allows to provide a specific localization of nanoparticles, offering the opportunity to image a whole animal. In addition, this approach enables also the determination of SLN accumulation in specific isolated organs [22].

In Figs. 7 and 8, a selection of the acquired images is shown, respectively referring to whole animals and isolated organs. In particular mice were treated with: (i) intraperitoneal injection of fluorescent SLN/P80-CG (Fig. 7-8A); (ii) intranasal administration of fluorescent SLN/P80-CG (Fig. 7-8B) or (iii) intraperitoneal injection of non fluorescent SLN/P80-e (Fig. 7-8C), employed as control for background reasons.

Photographs reported in Fig. 7 A, referring to an animal administered through the intraperitoneal route with SLN/P80-CG nanoparticles, show a diffuse fluorescence, particularly localized in liver and spleen regions. The animal imaged in Panel B, treated by intranasal route, shows a weaken signal with respect to that of panel A. It should be considered that the amount of SLN/P80-CG nanoparticles administered by intranasal administration was 10 fold lower with respect to the amount of nanoparticles injected by intraperitoneal administration.

The control mouse treated with the non fluorescent SLN/P80-e, imaged in panel C, as expected displays a very low signal.

Moreover different organs were isolated in order to investigate the distribution of SLN/P80-CG in organs and to univocally localize the fluorescent dye accumulated in specific districts. It is to be underlined that all organs were imaged after complete perfusion, with the aim to remove possible traces of fluorescence from the vasculature.

Fig. 8 shows the images of organs isolated from representative animals. In the case of intraperitoneal administration (Fig. 8A) (500 μl/animal) the fluorescent signal was observable in all isolated organs, with a predominant accumulation

in the liver and in the spleen, typical storage organs for nanoparticles [46, 47]. Fluorescence was also detectable in other organs, such as lung, kidney and brain. In the case of intranasal administration (Fig. 8B), it is noteworthy that in spite of the much smaller administered volume of SLN/P80-CG (50 μl/animal), the fluorescence signal was detectable not only in the nasal region (as expected) but also in liver, spleen and kidneys; interestingly, some spots of fluorescent signals were observable in the brain too.

In order to investigate comparatively the amount of nanoparticle reaching the brain after intraperitoneal or intranasal administration, a quantitative analysis of the fluorescent signals present in the brain tissue was performed. Fig. 9 shows that the fluorescence intensity in brain, after intraperitoneal injection is larger ($p<0.188$) than that detectable after intranasal administration. In addition, data indicate that the signals deriving from fluorescent particles are in all cases (apart from intranasal in isolated brains) statistically different from those obtained from the brains of mice treated with SLN/P80-e (used as control).

These results suggest that, despite the typical tropism of lipid nanoparticles for RES district, the produced SLN/P80 are able to reach the brain, even if in different extent, when intraperitoneal or intranasal administered.

The precise quantification of nanoparticle reaching the brain (with respect to the total admimistered dose), together with the analysis of accumulation of nanoparticles in specific brain regions, will be investigated in due course in programmed experiments.

4. Conclusions

The presented data indicate that DMF can be conveniently and efficiently encapsulated in SLN with dimensional and morphological properties well suitable for clinical applications requiring different administration routes.

The *in vitro* permeability experiments show that SLN, particularly those containing the positively charge surfactant DDAC, display an appreciable ability

to deliver the drug through the *in vitro* simulated BBB by bEnd.3 cell monolayers. Noteworthy are the *in vivo* biodistribution results relative to the intraperitoneal administration of SLN/P80-CG, these nanoparticles displayed indeed the capacity to pass BBB *in vivo*, as proven by the signal clearly detectable by fluorescence luminescent imaging.

With respect to the suitability of DMF loaded SLN for therapeutic use in MS treatment, the following aspects can be considered.

The dosage of Tecfidera is 120 mg/capsule; our SLN contain 6.6 mg/ml of DMF. Therefore, a reasonable administration of 2-5 ml of SLN dispersion would contain about 4-10 fold lower amount of DMF for a single dose.

Considering that SLN could allow a significant improvement of drug absorption and the avoidance of first-pass effects, it can be concluded that the proposed SLN contain an amount of DMF suitable for a therapeutic purpose.

Taken together the results described in the current paper represent a promising starting point for the further development of a DMF formulation based on SLN for the treatment of MS.

Acknowledgements: This work was funded by "FIRB 2010. Fondo per gli Investimenti della Ricerca di Base" from the Ministry of the University and Research of Italy (code RBFR10XKHS).

References

[1] A. Compston, A. Coles, Multiple sclerosis, Lancet, 372 (2008) 1502-17.

[2] A.M. Papini, E. König, Novel diagnostic tools and solutions for multiple sclerosis treatment: a patent review (2009-2014), Expert Opin Ther Pat, 8 (2015) 1-12.

[3] A.P. Robinson, C.T. Harp, A. Noronha, S.D. Miller, The experimental autoimmune encephalomyelitis (EAE) model of MS. utility for understanding disease pathophysiology and treatment. In Multiple Sclerosis and Related Disorders, Handbook of Clinical Neurology, 122 (2014) 173-1891.

[4] R.R. Gold, R.A. Linker, M. Stangel, Fumaric acid and its esters: an emerging treatment for multiple sclerosis with antioxidative mechanism of action, Clin Immunol, 142 (2012) 44-48.

[5] R. Bomprezzi, Dimethyl fumarate in the treatment of relapsing–remitting multiple sclerosis: an overview, Ther Adv Neurol Disord. 8 (2015) 20-30.

[6] M. Hutchinson, R.J. Fox, D.H. Miller, J.T. Phillips, M. Kita, E. Havrdova, J. O'Gorman, R. Zhang, M. Novas, V. Viglietta, K.T. Dawson, Clinical efficacy of BG-12 (dimethyl fumarate) in patients with relapsing-remitting multiple sclerosis: subgroup analyses of the CONFIRM study, J Neurol, 260 (2013) 2286-96.

[7] R.A. Linker, R. Gold, Dimethyl fumarate for treatment of multiple sclerosis: mechanism of action, effectiveness and side effects. Curr Neurol Neurosci Rep, 13 (2013) 394.

[8] A. Giusti, M. Giambuzzi, Management of dysphagia in patients affected by multiple sclerosis: state of the art, Neurol Sci, 29 (2008) S364-S366.

[9] M.D. Joshi, R.H. Müller, Lipid nanoparticles for parenteral delivery of actives, Eur J Pharm Biopharm, 71 (2009) 161-172.

[10] L. Battaglia, M. Gallarate, Lipid nanoparticles: state of the art, new preparation methods and challenges in drug delivery, Expert Opin Drug Deliv, 9 (2012) 497-508.

[11] B. Sriramoju, R.K. Kanwar, J.R. Kanwar, Nanomedicine based nanoparticles for neurological disorders, Curr Med Chem, 21 (2014): 4154-68.
[12] H. Gao, Z. Pang, X. Jiang, Targeted delivery of nano-therapeutics for major disorders of the central nervous system, Pharm Res, 30 (2013) 2485-98.
[13] J-C. Olivier, Drug Transport to Brain with Targeted Nanoparticles, NeuroRx,; 2 (2005) 108-119.
[14] J. Kreuter, Nanoparticulate systems for brain delivery of drugs, Adv Drug Deliv Rev, 47 (2001) 65-81.
[15] S. Duchi, H. Ovadia, E. Touitou, Nasal administration of drugs as a new non-invasive strategy for efficient treatment of multiple sclerosis. J Neuroimmunol, 258 (2013) 32-40.
[16] A. Pires, A. Fortuna, G. Alves, A. Falcão, Intranasal drug delivery: how, why and what for?, J Pharm Pharmaceut Sci, 12 (2009) 288-311.[17] X.H. Tian, X.N Lin, F. Wei, Z.C. Huang, P. Wang, L. Ren, Y. Diao, Enhanced brain targeting of temozolomide in polysorbate-80 coated polybutylcyanoacrylate nanoparticles, Int J Nanomed, 6 (2011) 445-452.
[18] M. Uner, G. Yener, Importance of solid lipid nanoparticles (SLN) in various administration routes and future perspectives, Int J Nanomed, 2 (2007) 289-300.
[19] P. R. Lockman, J. M. Koziara, R. J. Mumper, D. D. Allen, Nanoparticle surface charges alter blood–brain barrier integrity and permeability, J Drug Target, 12 (2004) 635-641.
[20] Y. Jallouli, A. Paillard, J. Chang, E. Sevin, D. Betbeder, Influence of surface charge and inner composition of porous nanoparticles to cross blood-brain barrier in vitro, Int J Pharm, 344 (2007) 103-109.
[21] E. Esposito, H. E. De Vries, S. M.A. Van Der Pol, F. Boschi, L. Calderan, S. Mannucci, M. Drechsler, C. Contado, R. Cortesi, C. Nastruzzi Production, Physico-Chemical Characterization and Biodistribution Studies of Lipid Nanoparticles. J Nanomed Nanotechnol, 6 (2015) 1-9.

[22] E. Esposito, M. Drechsler, R.Cortesi, C. Nastruzzi, Encapsulation of cannabinoid drugs in nanostructured lipid carriers. Eur J Pharm Biopharm, 102 (2016) 87-91.

[23] E. Esposito, P. Mariani, L. Ravani, C. Contado, M. Volta, S. Bido, M. Drechsler, M. Mazzoni, E. Menegatti, M. Morari, R. Cortesi, Nanoparticulate lipid dispersions for bromocriptine delivery: characterization and *in vivo* study, Eur J Pharm Biopharm, 80 (2012) 306-314.

[24] R. Pecora, Dynamic Light Scattering Measurement of Nanometer Particles in Liquids, J Nanoparticle Res, 2 (2000) 123-131.

[25] E. Esposito, L. Ravani, P. Mariani, N. Huang, P. Boldrini, M. Drechsler, G. Valacchi, R. Cortesi, C. Puglia. Effect of nanostructured lipid vehicles on percutaneous absorption of curcumin, Eur J Pharm Biopharm, 86 (2014) 121-132.

[26] E. Esposito, S. Mazzitelli, R. Cortesi, M. Drechsler, L. Ravani, C. Nastruzzi, Analysis of the drug release profiles from formulations based on micro and nano systems. Curr. Anal. Chem. 9 (2013) 37- 46.

[27] L.C. Herrera, M.V. Defain Tesoriero, L.G. Hermida, In Vitro Release Testing of PLGA Microspheres with Franz Diffusion Cells. Dissolution Technol, 5 (2012) 6-11.

[28] E. Esposito, L. Ravani, P. Mariani, C. Contado, M. Drechsler, C. Puglia, R. Cortesi, Curcumin containing monoolein aqueous dispersions: a preformulative study, Mat Sci Eng C, 33 (2013) 4923,4934.

[29] N.A. Peppas, Analysis of Fickian and non-Fickian drug release from polymers, Pharm Acta Helv 60 (1985) 110-111.

[30] J. Siepmann, F. Siepmann, Mathematical modeling of drug delivery, Int J Pharm, 364 (2008) 328-343.

General notices and requirements. Applying to Standards, Tests, Assays, and Other Specifications of the United States Pharmacopeia (2011) 1-14.

[34] S.A. Wissing, O. Kayser, R.H. Muller, Solid lipid nanoparticles for parenteral drug delivery, Adv Drug Delivery Rev, 56 (2004)1257-12722.

[35] T.M. Göppert, R.H. Müller, Polysorbate-stabilized solid lipid nanoparticles as colloidal carriers for intravenous targeting of drugs to the brain: comparison of plasma protein adsorption patterns, J Drug Target, 13 (2005) 179-187.
[36] M.L. Amin, P-glycoprotein inhibition for optimal drug delivery, Drug Target Insights, 7 (2013) 27-34.
[37] A. Ambruosi, H. Yamamoto, J. Kreuter, Body distribution of polysorbate-80 and doxorubicin-loaded [14C]poly(butyl cyanoacrylate) nanoparticles after i.v. administration in rats, J Drug Target, 13 (2005) 535-542.
[38] J.E. Hardebo, J. Kahrstrom, Endothelial negative surface charge areas and blood–brain barrier function, Acta Physiol Scand, 125 (1985) 495-499.

[39] M.N. Hart, L.F. VanDyk, S.A. Moore, D.M. Shasby, P.A. Cancilla, Differential opening of the brain endothelial barrier following neutralization of the endothelial luminal anionic charge in vitro, J Neuropathol Exp Neurol, 46 (1987) 141–153.

[40] A.W. Vorbrodt, Demonstration of anionic sites on the luminal and abluminal fronts of endothelial cells with poly-L-lysine-gold complex, J Histochem Cytochem 35 (1987) 1261-1266.[41] L. Fenart, A. Casanova, B. Dehouck, C. Duhem, S. Slupek, R. Cecchelli, D. Betbeder, Evaluation of effect of charge and lipid coating on ability of 60-nm nanoparticles to cross an in vitro model of the blood–brain barrier, J Pharmacol Exp Ther, 291 (1999) 1017-1022.
[42] K. Sato, Crystallization behaviour of fats and lipids: a review, Chemical Engineering Science 56 (2001) 2255-2265.
[43] E. Esposito, L. Ravani, M. Drechsler, P. Mariani, C. Contado, J. Ruokolainen, P. Ratano, P. Campolongo, V. Trezza, C. Nastruzzi, R. Cortesi, Cannabinoid antagonist in nanostructured lipid carriers (NLC): design, characterization and *in vivo* study, Mat. Sci. Eng. C 48 (2015) 328-336.
[44] G. Li, B.M. Fu, An electrodiffusion model for the blood-brain barrier permeability to charged molecules, J Biomech Eng, 133 (2011) 0210021-02100212.

[45] W. Yuan, G. Li, E.S. Gil, T.L. Lowe, B.M. Fu, Effect of surface charge of immortalized mouse cerebral endothelial cell monolayer on transport of charged solutes, Ann Biomed Eng, 38 (2010) 1463-72.
[46] E. Esposito, A. Boschi, L. Ravani, R. Cortesi, M. Drechsler, P. Mariani, S. Moscatelli, C. Contado, G. Di Domenico, C. Nastruzzi, M. Giganti, L. Uccelli, Biodistribution of nanostructured lipid carriers: a tomographic study, Eur J Pharm Biopharm, 89 (2015) 145-156.
[47] J.P.M. Almeida, A.L Chen, A. Foster, R. Drezek, *In vivo* biodistribution of nanoparticles. Nanomedicine, 6 (2011) 815-835.

Figure legends

Figure 1: Macroscopic analysis of SLN, SLN/P80 and SLN/DDAC produced in the absence (left) and in the presence (right) of DMF.
Cryo-TEM analysis of the indicated SLN formulations with different composition in the absence and in the presence of DMF. Bar corresponds to 200 nm. For nanoparticle acronym, composition and preparation procedure, please refer to Table 2 and experimental section.

Figure 2 A: Effect of the composition and DMF presence on SLN mean diameters (expressed as Z-Average, grey bars), and size distribution (expressed as dispersity, green bars), as determined by photon correlation spectroscopy. B: Effect of the composition and DMF presence on SLN recovery (grey bars), and presence of lipid agglomerates (blu bars). Data are the mean of 4 experiments ± S.D.. For nanoparticle acronym, composition and preparation procedure, please refer to Table 2 and experimental section.

Figure 3: Variation of Z Average mean diameters of SLN after 0 (plain bars), 3 (grey bars), and 6 (black bars), months from preparation, as determined by PCS. Data are the mean of 3 determinations ± S.D.. For nanoparticle acronym, composition and preparation procedure, please refer to Table 2 and experimental section.

Figure 4: In vitro release kinetics of DMF from SLN-DMF (●), SLN/P80-DMF (■) and SLN/DDAC-DMF (♦). Experiments were performed by Franz cell method. For comparison, the profile obtained using the free DMF solubilized in water is also reported (x). Data are the mean of 6 experiments ± S.D.. For nanoparticle acronym, composition and preparation procedure, please refer to Table 2 and experimental section.

Figure 5: Comparison of the theoretical (dotted lines) and experimental (solid lines) DMF profiles from SLN-DMF (A), SLN/P80-DMF (B) and SLN/DDAC-DMF (C). The theoretical curves were obtained using the coefficient calculated by linear regression of the linearized form of equation (3) (diamonds) and equation (4) (squares). For nanoparticle acronym, composition and preparation procedure, please refer to Table 2 and experimental section.

Figure 6: Effect of the SLN composition on the *in vitro* permeability. Data represent the mean of 3 experiments ± S.D.. Data refer to the permeability of the indicated SLN formulations. For nanoparticle acronym, composition and preparation procedure, please refer to Table 2 and experimental section.

Figure 7: Fluorescent luminescent imaging of SLN/P80-CG administered to athimic mice by intraperitoneal injection (A) or intranasal (B). Images were recorded after 4 h from the administration. Panel C reports the image of a control animal treated with non fluorescent SLN/P80-e administered by intraperitoneal injection. The color bar on the right side indicates the signal efficiency of the fluorescence emission coming out from the animal.

Figure 8: Distribution of SLN/P80-CG, as determined by fluorescent luminescent imaging on isolated organs 4 hours after administration: liver (a); brain (b); lungs (c); kidneys (d); spleen (e); brown fat (f). SLN/P80-CG were administered by intraperitoneal injection (A) or intranasal (B). In panel C are reported the images of control organs isolated from animals treated with non fluorescent SLN/P80-e administered by intraperitoneal injection. The color bar on the right side indicates the signal efficiency of the fluorescence emission coming out from the organ.

Figure 9: Quantitative analysis of the distribution of SLN/P80-CG *in vivo* and isolated brains. Black bars: intraperitoneal injection; grey bars: intranasal administration; for comparison the fluorescence intensity of mice treated with SLN/P80-e is also reported (plain bars) (* = p <0.003, ** = p <0.188).

Table(s)

Table 1: Physico-chemical characteristics and solubility of dimethyl fumarate

Physico-chemical parameters			
MW (g/mol)	144.13		
Melting point (°C)	102-106		
Boiling point (°C)	192-193		
Solubility (mg/ml)			
water	1.58		
water/ethanol (v/v)	50:50	80:20	90:10
	10.5	1.65	1.59
ethanol	16.22		
P80*/EtOH (v/v)	80:20	90:10	
	1.66	1.60	

*Aqueous solution of polysorbate 80 1% w/w

Table 2: Identification code, typical composition, Z average mean diameters and encapsulation efficiency of SLN employed in this study

acronym	*tristearin[a] (mg)*	*DDAC[b] (mg)*	*DMF[c] (mg)*	*RH[d] (mg)*	*CG[e] (mg)*	*P80[f]*	*Z average (nm)*	*DMF EE[g] (%)*
SLN-e	250	-	-	-	-	no	212.1±19	-
SLN-DMF	250	-	5	-	-	no	254.0±28	85.2±1.1
SLN/P80-e	250	-	-	-	-	yes	262.5±25	-
SLN/P80-DMF	250	-	5	-	-	yes	322.1±5	86.9±5.5
SLN/DDAC-e	200	50	-	-	-	no	185.2±15	-
SLN/DDAC-DMF	200	50	5	-	-	no	199.0±17	85.4±2.6
SLN-RH	250	-	-	1	-	no	185.3±15	-
SLN/P80-RH	250	-	-	1	-	yes	190.4±10	-
SLN/DDAC-RH	200	50	-	1	-	no	180.2±8	-
SLN-CG	250	-	-	-	1	no	172.6±7	-
SLN/P80-CG	250	-	-	-	1	yes	183.4±11	-

The aqueous phase was always 4.75 ml of poloxamer 188 2.5% w/w
[a]Glyceril tristearate
[b]Dioctadecyl dimethylammonium chloride
[c]Dimethyl fumarate
[d]Rhodamine
[e]Cardiogreen
[f]Polysorbate 80 post-production treatment
[g]Percentage (w/w) of DMF in SLN with respect to the total amount used for the preparation.
Data are the means ± SD of 6 independent determinations.

Table 3: Effect of DMF concentration on SLN recovery and drug encapsulation parameters

DMF (μg/mg lipid phase) [a]	*Recovery (%)*[b]	*Agglomerates (%)*[c]	*EE*[d] *(%)*	*LC*[e] *(%)*
20	95.5±2.5	5.51±2.0	85.2±1.1	0.34±0.1
40	85.3±2.1	13.11±3.1	80.2±1.3	0.64±0.2
60	72.4±3.4	26.4±4.2	53.4±1.5	0.64±0.1
80	52.0±4.5	47.16±5.7	33.4±2.8	0.40±0.1

[a]The amount of drug initially included in the lipid phase
[b]Percent of recovery was calculated as follows: % recovery = amount of SLN recovered (g)/amount of lipid used (g) x 100.
[c]Loss of lipids (lipid phase) due to the partial coalescence of the lipid phase during the formation of the O/W emulsion. Data represent the mean ± SD of 6 independent experiments.
[d]Percentage (w/w) of drug in SLN with respect to the total amount used for the preparation.
[e]Percentage (w/w) of drug in SLN with respect to the amount of lipid used for the preparation. Data represent the mean ± SD of 6 independent experiments.

Table 4: Kinetic parameters of DMF release from SLN

	Dissolutive parameter[a]			Diffusive parameter[b]		
Nanoparticle acronym	*K*	*c*	*R*	*K*	*c*	*R*
SLN-DMF	-0.27936	4.5488	0.9896	34.032	-1.8237	0.9955
SLN/P80-DMF	-0.35234	4.5878	0.9977	38.855	-4.3067	0.9862
SLN/DDAC-DMF	-0.29422	4.5485	0.9913	35.074	-1.812	0.9962

[a]As determined by equation (3)
[b]As determined by equation (4)

Figure(s)

Click here to download high resolution image

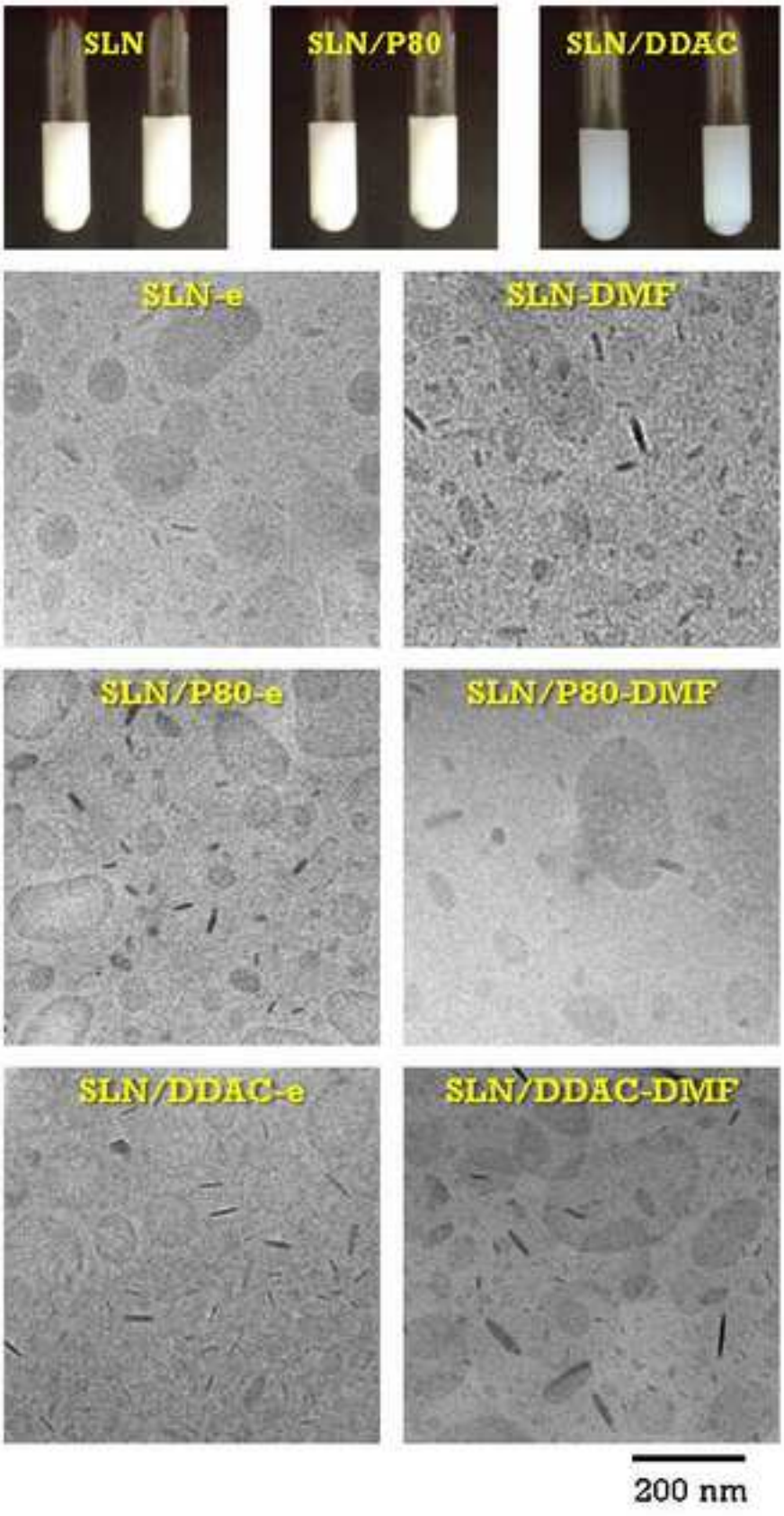

Figure(s)

Click here to download high resolution image

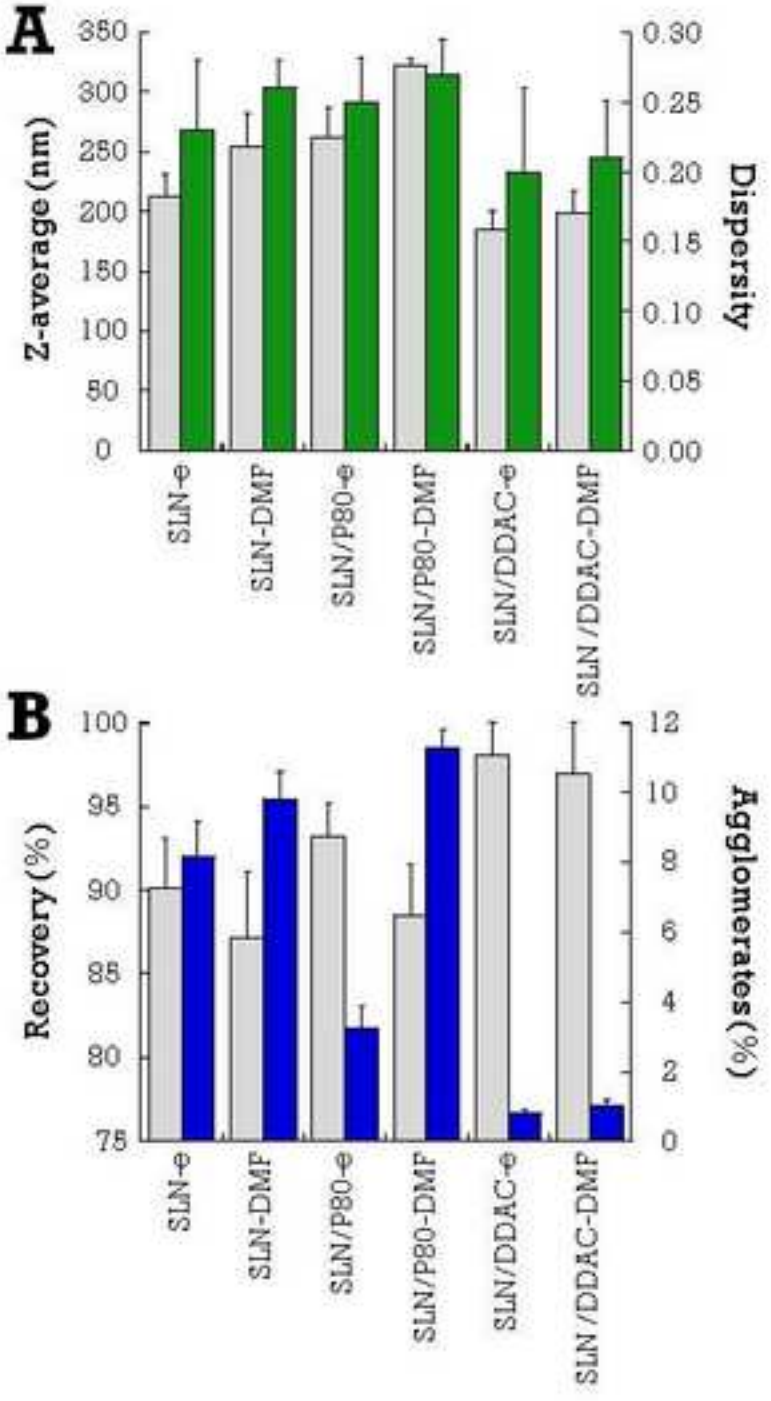

Figure(s)

Click here to download high resolution image

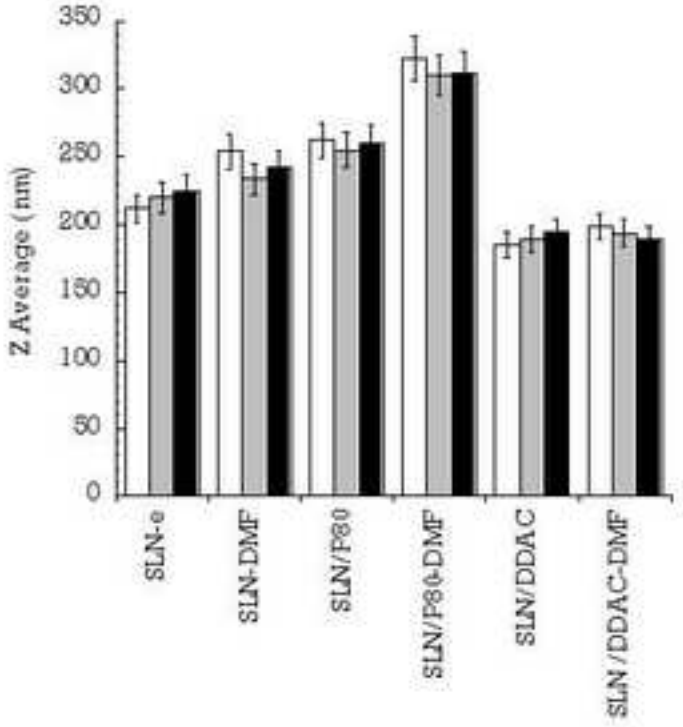

Figure(s)

Click here to download high resolution image

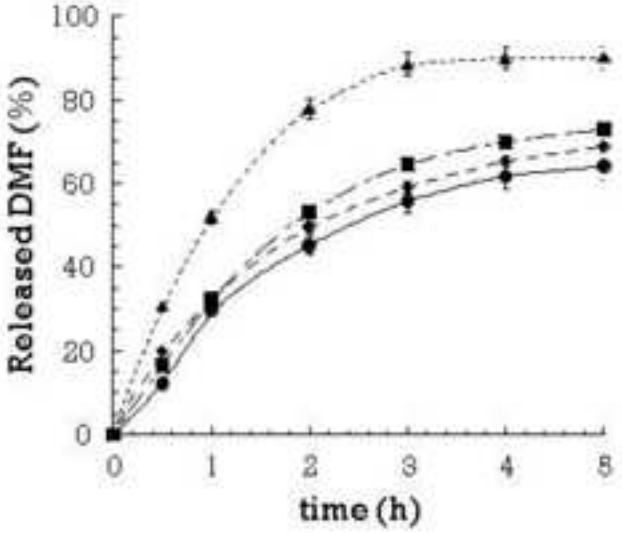

Figure(s)

Click here to download high resolution image

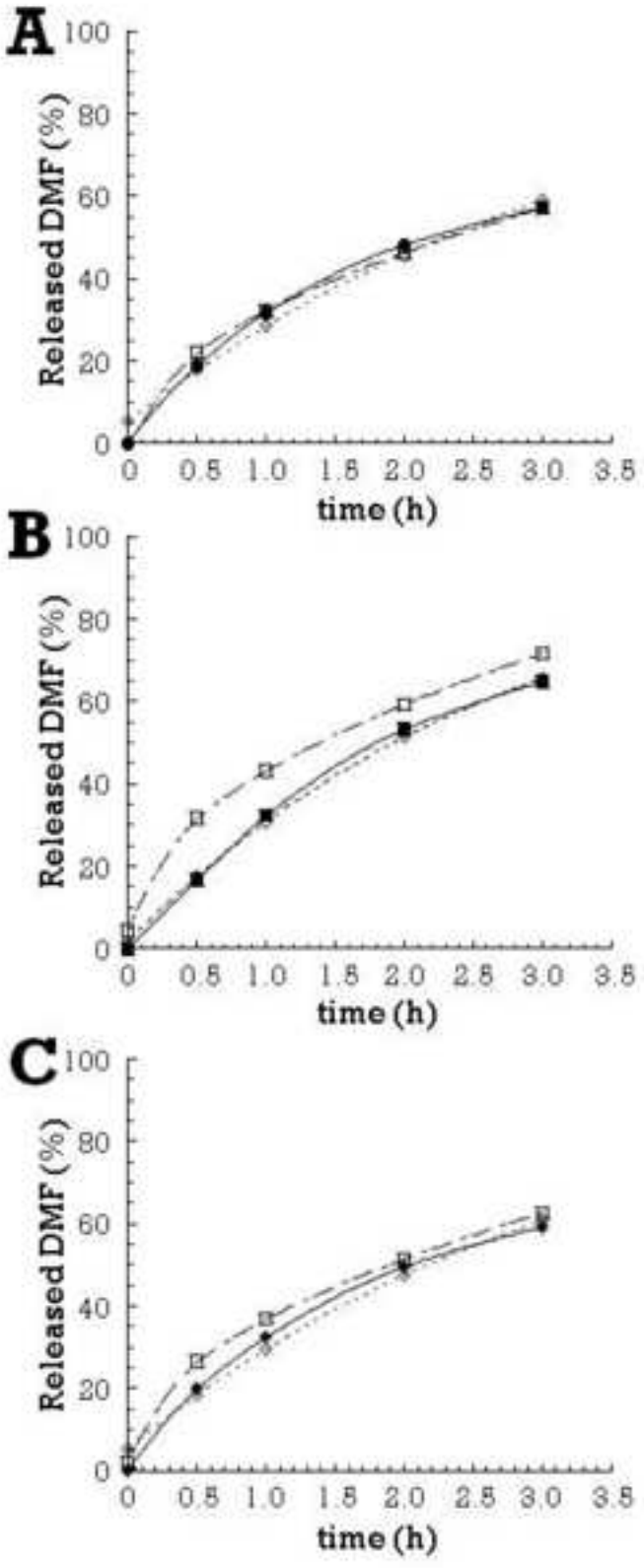

Figure(s)

Click here to download high resolution image

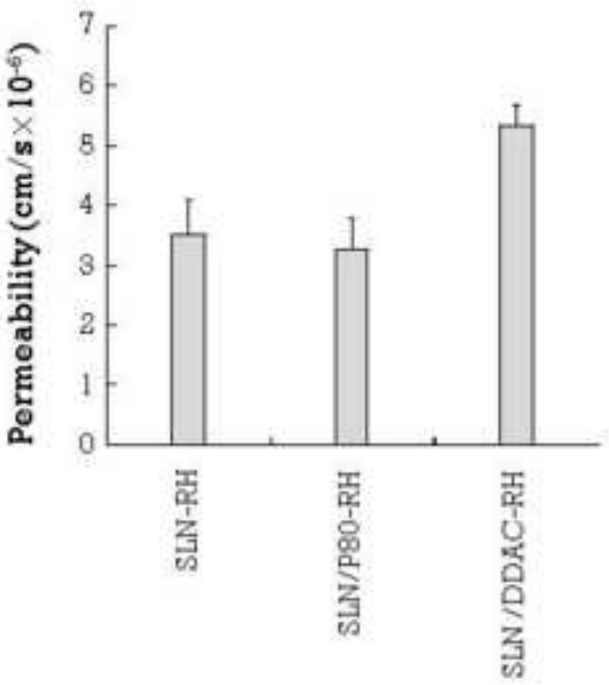

Figure(s)

Click here to download high resolution image

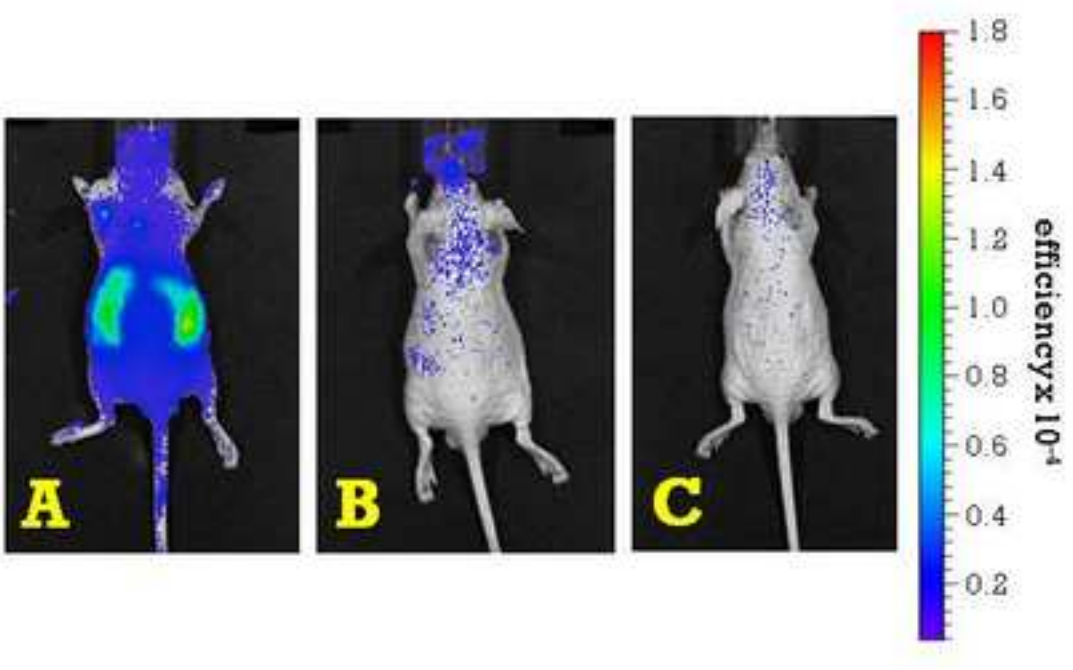

Figure(s)

Click here to download high resolution image

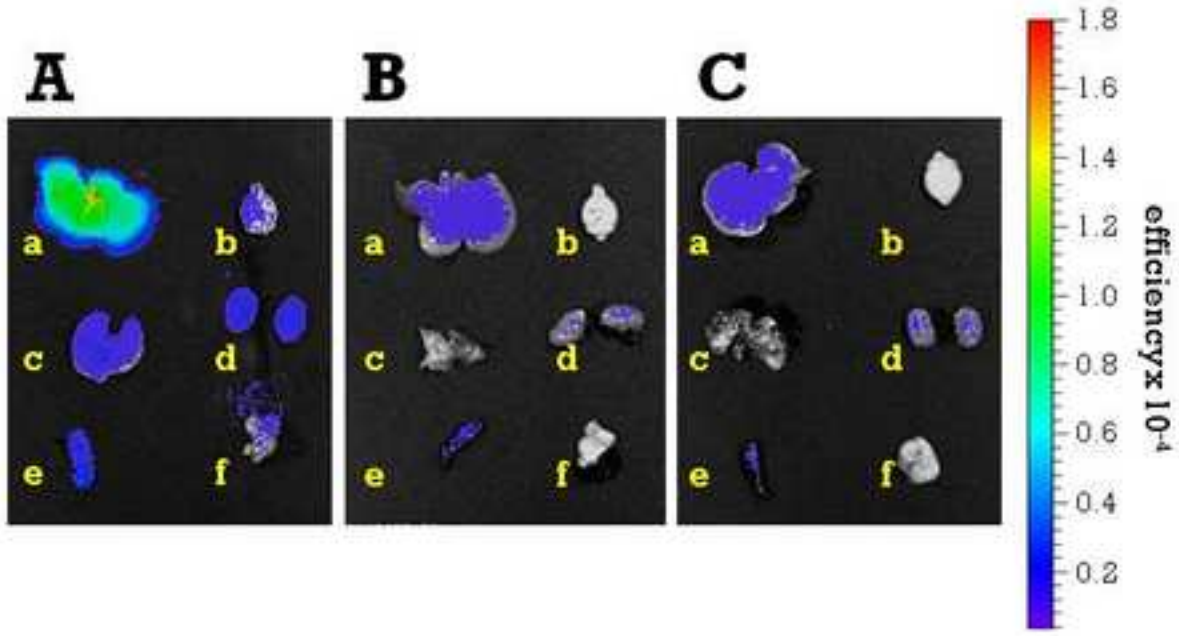

Figure(s)

Click here to download high resolution image